Naval Research Laboratory

Washington, DC 20375-5320

NRL/MR/5650--08-9161

Analysis of Analog Photonic Links Employing Multiple-Channel (Arrayed) Receivers

JASON D. MCKINNEY
VINCENT J. URICK
FRANK BUCHOLTZ
CARL VILLARRUEL

Photonics Technology Branch
Optical Sciences Division

CHRISTOPHER SUNDERMAN

Global Strategies Group
Crofton, Maryland

November 7, 2008

Approved for public release; distribution is unlimited.

REPORT DOCUMENTATION PAGE

Form Approved
OMB No. 0704-0188

Public reporting burden for this collection of information is estimated to average 1 hour per response, including the time for reviewing instructions, searching existing data sources, gathering and maintaining the data needed, and completing and reviewing this collection of information. Send comments regarding this burden estimate or any other aspect of this collection of information, including suggestions for reducing this burden to Department of Defense, Washington Headquarters Services, Directorate for Information Operations and Reports (0704-0188), 1215 Jefferson Davis Highway, Suite 1204, Arlington, VA 22202-4302. Respondents should be aware that notwithstanding any other provision of law, no person shall be subject to any penalty for failing to comply with a collection of information if it does not display a currently valid OMB control number. **PLEASE DO NOT RETURN YOUR FORM TO THE ABOVE ADDRESS.**

1. REPORT DATE *(DD-MM-YYYY)*	**2. REPORT TYPE**	**3. DATES COVERED** *(From - To)*
07-11-2008	Memorandum Report	01-04-08 – 30-09-2008

4. TITLE AND SUBTITLE

Analysis of Analog Photonic Links Employing Multiple-Channel (Arrayed) Receivers

5a. CONTRACT NUMBER

5b. GRANT NUMBER

5c. PROGRAM ELEMENT NUMBER

6. AUTHOR(S)

Jason D. McKinney, Vincent J. Urick, Frank Bucholtz,
Carl Villarruel, and Christopher Sunderman*

5d. PROJECT NUMBER

5e. TASK NUMBER

5f. WORK UNIT NUMBER

7. PERFORMING ORGANIZATION NAME(S) AND ADDRESS(ES)

Naval Research Laboratory, Code 5650
4555 Overlook Avenue, SW
Washington, DC 20375-5320

8. PERFORMING ORGANIZATION REPORT NUMBER

NRL/MR/5650--08-9161

9. SPONSORING / MONITORING AGENCY NAME(S) AND ADDRESS(ES)

Office of Naval Research
875 North Randolph St.
Arlington, VA 22203-1995

10. SPONSOR / MONITOR'S ACRONYM(S)

ONR

11. SPONSOR / MONITOR'S REPORT NUMBER(S)

12. DISTRIBUTION / AVAILABILITY STATEMENT

Approved for public release; distribution is unlimited.

13. SUPPLEMENTARY NOTES

*Global Strategies Group, Crofton, MD

14. ABSTRACT

Analog photonic links have seen increased application to military systems in recent years. While virtually all deployed systems utilize optical fiber as the transmission medium, for example in antenna remoting applications, there is increased interest in applying these links in free-space applications. For free-space systems, the received optical power may be significantly below that in fiber-based applications; this necessitates new receiver and amplification architectures to obtain the required receiver sensitivity. One solution is the use of arrayed receivers, i.e., those employing multiple receive channels (analogous to the use of phased arrays in radar systems), each with an optical amplifier to boost the received optical signal level. While analog links utilizing single-channel and balanced receivers have been thoroughly analyzed, arrayed receiver architectures have received far less attention. In this work, we provide a complete noise analysis of multiple-channel receivers employing optical amplifiers and provide experimental verification of the achievable increase in sensitivity of these architectures.

15. SUBJECT TERMS

Analog optical links Arrayed receivers
Noise figure

16. SECURITY CLASSIFICATION OF:			**17. LIMITATION OF ABSTRACT**	**18. NUMBER OF PAGES**	**19a. NAME OF RESPONSIBLE PERSON**
a. REPORT	**b. ABSTRACT**	**c. THIS PAGE**			Jason D. McKinney
Unclassified	Unclassified	Unclassified	UL	27	**19b. TELEPHONE NUMBER** *(include area code)* (202) 404-4207

Standard Form 298 (Rev. 8-98)
Prescribed by ANSI Std. Z39.18

CONTENTS

I EXECUTIVE SUMMARY

Analog photonic links have seen increased application to military systems in recent years. While virtually all deployed systems utilize optical fiber as the transmission medium, for example in antenna remoting applications, there is increased interest in applying these links in free-space applications. For free-space systems, the received optical power may be significantly below that in fiber-based applications; this necessitates new receiver and amplification architectures to obtain the required receiver sensitivity. One solution is the use of arrayed receivers, i.e., those employing multiple receive channels (analogous to the use of phased arrays in radar systems), each with an optical amplifier to boost the received optical signal level. While analog links utilizing single-channel and balanced receivers have been thoroughly analyzed, arrayed receiver architectures have received far less attention. In this work we provide a complete noise analysis of multiple-channel receivers employing optical amplifiers and provide experimental verification of the achievable increase in sensitivity of these architectures. This work:

- Provides general expressions for the RF gain and noise figure of arrayed receivers;
- Gives a generalized expression for the noise penalty incurred by the use of optical amplifiers in an analog photonic link;
- Provides experimental verification of the array gain and sensitivity improvement achieved via arrayed receivers utilizing optical amplifiers (specifically, erbium-doped fiber amplifiers);
- Provides simulation code to predict the gain and noise figure of an NxN channel arrayed receiver.

ANALYSIS OF ANALOG PHOTONIC LINKS EMPLOYING MULTIPLE-CHANNEL (ARRAYED) RECEIVERS

II INTRODUCTION

Analog optical links are finding increased application in commercial and military systems ranging from radio-over-fiber applications [1], antenna remoting [2, 3], and optical signal processing [4]. For these fiber-based applications, single-diode receivers have been thoroughly described in the literature [5]. As the performance of an analog link improves with received photocurrent, optical amplifiers – predominantly erbium-doped fiber amplifiers (EDFAs) – have been readily incorporated into a variety of systems. It is well known that the addition of an optical amplifier (EDFA) raises the electrical noise floor in both digital and analog applications [6, 7] due to the presence of amplified spontaneous emission (optical) noise. To mitigate this additional noise in systems employing EDFAs prior to modulation, dual-output optical modulators and balanced-detection [8, 9] are frequently employed. This technique has been utilized alone to achieve the first multi-gigahertz bandwidth analog optical link with a noise figure < 10 dB [10] and in concert with other techniques to achieve an RF noise figure approaching 3 dB [11].

While pre-modulation amplification and balanced-detection may be utilized to approach shot noise-limited performance in an analog link, other techniques may be applied to increase the link gain (increase the received photocurrent) while also decreasing the effect of noise from the EDFA. In particular the analysis presented here considers arrayed-receivers – those employing multiple optical paths post-modulation and multiple photodiodes. In these architectures, the desired output RF photocurrent is recovered from each photodiode individually; the individual photocurrents are then coherently combined in the electrical domain. Conceptually, the operation of these receivers is analogous to a phased-array antenna operating in receive-mode [12] where the output of multiple antenna elements are combined in-phase to increased the signal-to-noise ratio of the received signal as compared to that from a single element. While such architectures, or their optical equivalents, have been widely explored for optical signal processing of microwave signals [4, 13], to the authors' knowledge these arrayed geometries have not received significant attention (or analysis) when used as phased receivers (with no intentional filtering). Such arrayed receivers could find widespread application, especially in analog systems utilizing free-space optical links.

In this work we analyze the performance of arrayed-receivers in which each optical (receiver) path employs an EDFA. In our analysis we derive general expressions for two of the primary RF performance metrics – gain and noise figure – of an analog link utilizing the arrayed-receiver concept. This analysis links the performance of the EDFAs utilized in the system to the RF noise figure. Specifically, this is achieved by extending the concept of the noise-penalty [7] associated with an EDFA – defined for a highly compressed amplifier – to all regimes of amplifier operation, in particular the linear amplification regime. We experimentally verify our analysis using two arrayed-receiver architectures that achieve signal combination in the electrical domain. While our demonstrations focus on electrically-combined receivers, the results of our analysis apply directly to incoherent optically-combined architectures [4].

This report is organized as follows. First, we derive the RF gain and noise figure for an analog link employing an N-channel electrically-combined receiver in Section III. This section includes the derivation of the generalized noise penalty of an EDFA. Section IV presents experimental demonstrations of two types of four-channel receivers and includes experimental characterization of the optical amplifiers utilized in the arrayed-receivers, as well as a discussion of the predicted receiver performance. In Section V we summarize our work. Appendix A (Sec. VIII) provides a short simulation (written in MATLAB) that calculates the gain and noise figure of an NxN arrayed receiver with user-defined channel weights, and Appendix B (Sec. IX)

Manuscript approved October 8, 2008.

analyzes the magnitude of the excess electrical noise arising from an EDFA.

III INTENSITY-MODULATED DIRECT-DETECTION ANALOG OPTICAL LINKS

In the externally intensity-modulated direct-detection (IMDD) analog optical link architecture, a continuous-wave (CW) laser is amplitude modulated with the desired RF input signal via a Mach-Zehnder intensity modulator (MZM). The Modulated optical signal is transmitted over some length of optical fiber (or, potentially free-space) and the RF signal is recovered at the distal end of the optical link through optical-to-electrical conversion with a high-speed photodiode. The typical (single-channel) externally-modulated IMDD architecture employing post-modulation amplification with an erbium-doped fiber amplifier (EDFA) is shown in Figure 1 (a). The focus of this work is to describe the noise performance of IMDD links employing multiple channel receivers; that is, receivers in which multiple optical or electronic signals are combined to obtain the RF output signal from the link. The schematic of such an architecture is shown in Fig. 1 (b). While the specific application motivating this work utilizes a free-space optical link between the modulator and EDFA, a standard IMDD link employing optical fiber between the modulator and amplifier provides a sound starting point for our analysis.

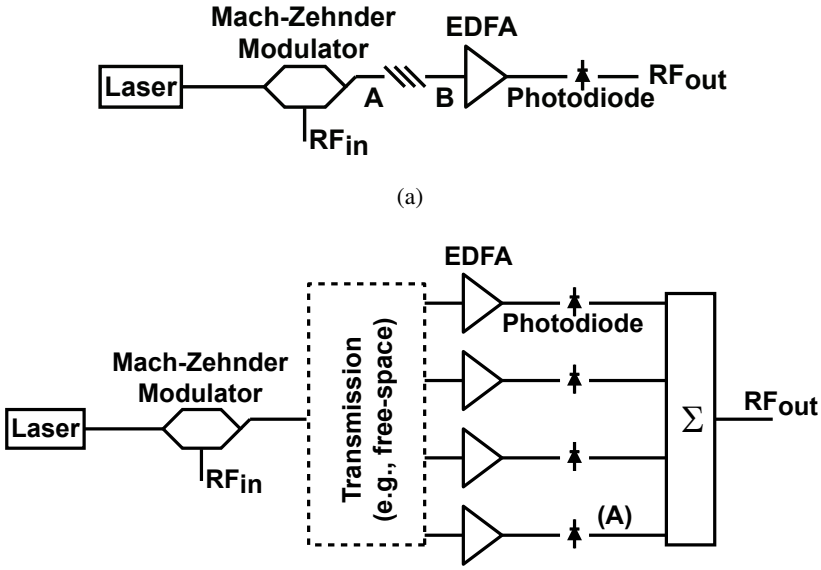

Fig. 1: (a) Single-channel intensity-modulated direct-detection RF photonic link. (b) Analog link employing a multiple-channel receiver.

Output Photocurrent and RF Gain in Electronically-Combined Multiple-Channel Receivers.

We begin with an expression for the output photocurrent from a single-diode IMDD analog link architecture. From the photocurrent we may then derive the various link metrics (gain, noise figure, and the like). Since the emphasis of this work is the noise performance of such links employing various optical or electrical signal combination geometries (and not linearity or dynamic range), we focus on the RF gain and noise figure for these architectures. We note, signal combination may be achieved in either the optical or electronic domains. In the optical domain, incoherent architectures (e.g. those employing a wavelength-division-multiplexing approach for multiple receive channels [4]) are preferable because optical phase variations

between channels do not affect the link performance. In these architectures the mathematics describing the RF performance of the link are identical to those describing a receiver employing electronic signal combination. In this work we emphasize electronically combined architectures - the analysis, however, may be directly applied to incoherent optically-combined receivers.

For a single-diode IMDD link with an RF input voltage $v_{\text{in}}(t) = v_{\text{rf}} \sin(\omega t)$, it may be readily shown [5, 7] the output photocurrent is given by the expression

$$i_{\text{out}}(t) = I_{\text{dc}} \left\{ 1 - \cos \left[\phi_b + \pi \frac{v_{\text{rf}}}{V_\pi(\omega)} \sin(\omega t) \right] \right\} + i_{\text{noise}}(t) \,. \tag{1}$$

In this expression, ϕ_b is the bias phase of the MZM, I_{dc} is the DC photocurrent at quadrature bias ($\phi_b = \pi/2$), $V_\pi(\omega)$ is the frequency-dependent halfwave voltage of the modulator, and $i_{\text{noise}}(t)$ is the noise current present in the link output (to be discussed later in this section). When the MZM is biased at quadrature ($\phi_b = \pi/2$) and the input RF signal satisfies the small-signal condition $|v_{\text{rf}}| \ll V_\pi(\omega)$ the link operates in the linear regime. In this mode of operation the photocurrent is well described by the linear small-angle approximation to Eq. (1),

$$i_{\text{out}}(t) = I_{\text{dc}} \left[1 - \pi \frac{v_{\text{rf}}}{V_\pi(\omega)} \sin(\omega t) \right] + i_{\text{noise}}(t) \,. \tag{2}$$

The emphasis of this work is to describe the noise performance of a photonic link comprising a single modulator and multiple parallel receive paths. The photocurrent from the composite link (composed of N parallel channels) may be written as

$$i_{\text{out}}(t) = \sum_{n=1}^{N} i_{\text{out,n}}(t) \,. \tag{3}$$

Here $i_{\text{out,n}}(t)$ is the photocurrent from channel n which, in the small-signal limit, is expressed as [from Eq. (2)]

$$i_{\text{out,n}}(t) = I_{\text{dc,n}} \left[1 - \pi \frac{v_{\text{rf}}}{V_\pi(\omega)} \sin(\omega t) \right] + i_{\text{noise,n}}(t) \,. \tag{4}$$

We see that the output photocurrent will consist of three terms: the total DC photocurrent, the total signal current [$i_{\text{out,n}}(t)$, oscillating at frequency ω] and the total noise photocurrent. We will first consider the total signal photocurrent; we will address the total noise photocurrent later in this section.

The total signal photocurrent may be expressed as

$$\begin{aligned} i_{\text{sig}}(t) &= \sum_{n=1}^{N} i_{\text{sig,n}}(t) \\ &= \pi I_{\text{dc,ref}} \frac{v_{\text{rf}}}{V_\pi(\omega)} \sin(\omega t) * \sum_{n=1}^{N} \alpha_n \delta(t - \tau_n) \,. \end{aligned} \tag{5}$$

In this expression, $I_{\text{dc,ref}}$ is the DC photocurrent of a reference channel [e.g. measured at point (A) in Fig. 1 (b)], α_n is the (real and positive-definite) weighting of channel n relative to the reference channel, $\delta(t - \tau_n)$ is the Dirac delta function representing a time delay of τ_n relative to the reference channel, and $*$ denotes convolution. We note that RF filters may be constructed by controlling the relative time-delay of each channel (tapped delay-line filters [4, 13]); here, however, we are interested in the case where all signals (at all RF frequencies) are combined in-phase (i.e. zero relative time-delay between channels). When all paths are delay-matched ($\tau_n = 0$ for all n), the total signal photocurrent is given by

$$i_{\text{sig}}(t) = \left(\sum_{n=1}^{N} \alpha_n \right) \pi I_{\text{dc,ref}} \frac{v_{\text{rf}}}{V_\pi(\omega)} \sin(\omega t) \,. \tag{6}$$

The time-average power at frequency ω delivered to a load resistance R_o is then given by

$$P_{\text{sig}}(\omega) = \left(\sum_{n=1}^{N} \alpha_n\right)^2 \left[\pi \frac{I_{\text{dc,ref}}}{V_\pi(\omega)}\right]^2 \frac{|v_{\text{rf}}|^2}{2} R_o. \tag{7}$$

Dividing the output RF power by the time-average input power $P_{\text{in}}(\omega) = 1/2R_i\,|v_{\text{rf}}|^2$ (R_i is the input resistance of the MZM) yields the RF power gain of the link

$$\begin{aligned} G_{\text{rf}}(\omega) &= \left(\sum_{n=1}^{N} \alpha_n\right)^2 \left\{\left[\pi \frac{I_{\text{dc,ref}}}{V_\pi(\omega)}\right]^2 R_i R_o\right\} \\ &= \left(\sum_{n=1}^{N} \alpha_n\right)^2 G_{\text{ref}}(\omega)\,. \end{aligned} \tag{8}$$

We see that the gain of the composite link is equal to the gain of the reference link [braced term in Eq. (8)] multiplied by a scaling factor [parenthetical term in Eq. (8)] which accounts for the coherent summation of the signal current from each channel in the receiver. We note the weighting factor $\alpha_n \leq 1$ accounts for any intentional channel weighting, excess per-channel loss, and any inherent coupling loss of the signal combiner. Therefore, the overall gain improvement [relative to the gain of the reference channel $G_{\text{ref}}(\omega)$] obtained by utilizing an N-channel receiver will strongly depend on the signal combination technique (e.g., waveguide combination or hard-wiring) utilized in the receiver. This dependence will be discussed further in the Experiment section of this report. In the following section we analyze the noise performance of the multiple-channel receiving architecture.

RF Noise Performance for IMDD Links Employing Multiple-Channel Receivers and Post-Modulation Optical Amplification

It is well known that the addition of an optical amplifier in the link architecture adds additional noise in the RF domain. Here we focus on erbium-doped fiber amplifiers (EDFAs) – though the general analysis may be applied to links employing semiconductor optical amplifiers, for example. The goal of this section is to express the electrical noise factor in terms of measurable characteristics of the EDFA employed in the optical link. We therefore begin with the definition of RF noise factor [14] – the ratio of input to output (power) signal-to-noise ratios (SNR)

$$\text{nf} = \frac{\text{SNR}_{\text{in}}}{\text{SNR}_{\text{out}}} = \frac{S_{\text{in}}}{N_{\text{in}}} \Big/ \frac{S_{\text{out}}}{N_{\text{out}}}, \tag{9}$$

under the assumption that the input SNR is limited by thermal noise (N_{th}). Here, S_{in} and S_{out} are the input and output signal powers; N_{in} and N_{out} are the total input and output noise power spectral densities, respectively. Since the output signal power is equal to that of the input multiplied by the power gain of the link, the noise factor may them be written in terms of the input ($N_{\text{in}} = N_{\text{th}}$) and output ($N_{\text{out}}$) noise power spectral densities (PSD, in W/Hz) and the link RF power gain

$$\text{nf} = \frac{1}{G_{\text{rf}}} \frac{N_{\text{out}}}{N_{\text{th}}}. \tag{10}$$

The output electrical noise power (W) from the link is given by

$$N_{\text{out}} \times B_e = \left(G_{\text{rf}} N_{\text{th}} + N_{\text{laser}} + N_{\text{th}} + N_{\text{shot, sig}} + N_{\text{excess}}\right) \times B_e. \tag{11}$$

In this expression, B_e is the electrical bandwidth of the receiver. The output noise power spectral density consists of five terms (from left to right): input thermal noise which sees the link gain, laser relative intensity noise (RIN), output thermal noise generated at the photodiode, shot noise generated by the photodetection process of the amplified laser, and the additional noise arising from the use of an EDFA. The first four terms are considered fundamental to the RF photonic link. The laser RIN is generally not easily expressed in closed form and is treated as a measured quantity in this work. While the additional noise arising from the EDFA (N_{excess}) may be expressed in terms of fundamental parameters of the amplifier [6], here we opt for a description based on measurable properties of the EDFA similar to that in [7]. Specifically we describe N_{excess} using a noise penalty – which may be written in terms of the gain and noise figure of the EDFA – relative to the ideal shot noise level. To simplify the discussion of arrayed receivers later in this section, we define the receiver noise PSD (added post-modulation) as

$$N_{\text{rx}} = N_{\text{th}} + N_{\text{shot, sig}} + N_{\text{excess}}. \tag{12}$$

Substituting this definition into Eq. (11), we may then write the total noise at the link output as

$$N_{\text{out}} \times B_e = (G_{\text{rf}} N_{\text{th}} + N_{\text{laser}} + N_{\text{rx}}) \times B_e. \tag{13}$$

To determine the RF noise figure of an analog link employing a post-modulator EDFA, we first need to determine the additional electrical noise added by the EDFA and express this quantity in terms of measurable parameters of the amplifier. In particular, we wish to express the additional noise in terms of the EDFA gain and noise factor. The definition of the optical noise factor follows the same general definition of Eq. (9) – it is the ratio of the electrical signal-to-noise ratios before and after the EDFA [6, 15]

$$\text{nf}_{\text{opt}} = \frac{\text{SNR}_{\text{in}}}{\text{SNR}_{\text{out}}}. \tag{14}$$

Here, the optical noise factor is defined relative to a shot-noise limited optical source [6] and the photocurrent is assumed to be measured with an ideal photodetector (unit quantum efficiency) [6, 15]. With these conditions the optical noise factor may be written as [15]

$$\text{nf}_{\text{opt}} = \frac{1}{G_{\text{opt}}} \left(1 + \frac{N_{\text{excess}}}{\alpha^2 R_o 2 h\nu G_{\text{opt}} P_{\text{in}}} \right). \tag{15}$$

Here, α is the DC responsivity (A/W) of the photodiode used to perform the measurement, R_o is the load resistance of the measurement device (spectrum analyzer, e.g.), G_{opt} is the EDFA gain, P_{in} is the optical power into the amplifier, h is Planck's constant, and ν is the optical frequency of the laser.

The term N_{excess} arises from the presence of amplified spontaneous emission noise (ASE) at the EDFA output. This term contains three components: signal-ASE beat noise, ASE-ASE beat noise and additional shot noise arising from the total ASE exiting the amplifier. Treatments of EDFA noise in the literature [15] lump this additional shot noise with that arising from the amplified laser (signal). When calculating the EDFA noise factor, or the RF noise factor of an analog link based on measured noise levels, this has no effect. When comparing the RF noise factor of an analog link to its "shot-noise limited" performance, treating the shot noise arising from ASE and that arising from the amplified laser as one quantity will lead to erroneous results as this calculation typically uses the measured DC photocurrent (not measured optical powers). To address this, we include the additional shot noise due to the total ASE power in the excess noise N_{excess}.

If we substitute the definition of the photodiode responsivity $\alpha = \eta q / (h\nu)$, where η is the diode's quantum efficiency (QE) into the Eq. (15), we may re-write the optical noise factor as

$$\text{nf}_{\text{opt}} = \frac{1}{G_{\text{opt}}} \left(1 + \frac{1}{\eta} \frac{N_{\text{excess}}}{N_{\text{sh,sig}}} \right). \tag{16}$$

Here we have used the definition of shot noise (W/Hz) [16]

$$N_{\text{shot, sig}} = 2qI_{\text{dc}}R_o, \tag{17}$$

with $I_{\text{dc}} = \alpha G_{\text{opt}} P_{\text{in}}$ equal to the DC photocurrent that would be measured at the EDFA output (using a photodiode with QE = η, and due entirely to the amplified laser). In this expression, q is the electronic charge and R_o is the load resistance seen by the photodiode.

We define the noise penalty (unitless) incurred by utilizing the EDFA to be the parenthetical term in Eq. (19)

$$\text{np} = \left(1 + \frac{1}{\eta}\frac{N_{\text{excess}}}{N_{\text{sh,out}}}\right). \tag{18}$$

With this definition, the optical noise factor may be expressed as

$$\text{nf}_{\text{opt}} = \frac{1}{G_{\text{opt}}} \times \text{np}. \tag{19}$$

Alternatively, the noise penalty incurred by using an EDFA may be expressed in terms of the optical gain and noise factor

$$\text{np} = G_{\text{opt}}\text{nf}_{\text{opt}}. \tag{20}$$

We note, the noise penalty as defined here assumes there is zero post-EDFA optical loss. In an actual analog link this idealization no longer holds – we will address this fact in the derivation of the RF noise factor below.

To determine the RF noise factor of the analog link (here, a single link), we start by substituting the total output noise [Eq. (11)] into the expression given by Eq. (10). For the purposes of this work we make the assumption that the laser RIN is negligible (N_{laser}=0); the noise factor is then given by

$$\text{nf} = 1 + \frac{1}{G_{\text{rf}}} + \frac{1}{G_{\text{rf}}}\frac{N'_{\text{shot, sig}}}{N_{\text{th}}}\left(1 + \frac{N'_{\text{excess}}}{N'_{\text{shot, sig}}}\right). \tag{21}$$

Here, the primed quantities are related to the corresponding quantities measured directly at the EDFA output by the post-amplifier loss ($\alpha_l \leq 1$) and the relations $N'_{\text{excess}} = \alpha_l^2 N_{\text{excess}}$ and $N'_{\text{shot, sig}} = \alpha_l N_{\text{shot, sig}}$. To simplify the inclusion of post-EDFA optical loss, we again consider the excess noise N_{excess}. As mentioned previously, this term contains signal-ASE beat noise, ASE-ASE beat noise and shot noise arising from the total ASE power. The first two terms decrease quadratically with post-amplifier optical loss (α_l) [7] because the RF noise PSD depends upon the product of the ASE power with either the power of the amplified laser (signal-ASE) or with itself (ASE-ASE) [6]. The shot noise term, however, decreases linearly with optical loss since it depends only on the total ASE power. An order-of-magnitude comparison (see Appendix B) reveals that the shot noise contribution to N_{excess} is roughly 10,000x lower than the sum of the beat noise components over the entire operating range of the EDFA. Therefore, the shot noise contribution to the excess noise may be safely ignored. With this simplification ratio $N'_{\text{excess}}/N'_{\text{shot, sig}}$ is related to the ratio of excess noise to shot noise at the EDFA output by [through Eq. (18)]

$$\frac{N'_{\text{edfa}}}{N'_{\text{shot, sig}}} = \alpha_l \frac{N_{\text{edfa}}}{N_{\text{shot, sig}}} = \eta\alpha_l\left(\text{np} - 1\right). \tag{22}$$

Substituting the above relation and the expression for the noise penalty given by Eq. (20) into Eq. (21) we obtain the RF noise factor in terms of the EDFA gain and noise factor (G_{opt} and nf_{opt}), photodiode quantum efficiency (η) and post-amplifier optical loss (α_l),

$$\text{nf} = 1 + \frac{1}{G_{\text{rf}}} + \frac{1}{G_{\text{rf}}}\frac{N'_{\text{shot, sig}}}{N_{\text{th}}}\left[(1 - \eta\alpha_l) + \eta\alpha_l G_{\text{opt}}\text{nf}_{\text{opt}}\right]. \tag{23}$$

Again, $N'_{\text{shot, sig}}$ is the shot noise arising from only the amplified laser, after any post-amplifier loss. In practice, if the EDFA is sufficiently saturated, or if an ASE-blocking filter is utilized post-amplifier, the shot noise will in fact be dominated by this quantity. The shot noise may then be calculated using the measured DC photocurrent using Eq. (17). If ASE contributes significantly to the total average optical power, the DC photocurrent must be reduced accordingly.

To determine the noise factor of the link employing a multiple-channel (arrayed) receiver, we must return to the noise photocurrent in Eqs. (1)-(4). Because the receiver noise current from each channel is independent of that of the other channels (in the absence of laser RIN or pre-modulation amplification), we may simply add the per-channel receiver noise powers [17]. If we take the frequency responses of all channels to be equal, the total receiver noise power spectral density (PSD) may be expressed as [from Eq. (12)]

$$N_{\text{rx,array}} = N_{\text{rx, ref}} \sum_{n=1}^{N} \alpha_n^2, \tag{24}$$

where $N_{\text{rx, ref}}$ is the receiver noise PSD of the reference channel. Substituting the total receiver noise PSD into the expression for the total noise PSD [Eq. (13)], and subsequently inserting to total output noise PSD and the gain of the composite link [Eq. (8)] into the general noise factor given in Eq. (10), we obtain

$$\begin{aligned} \text{nf}_{\text{array}} &= \frac{1}{G_{\text{rf}} N_{\text{th}}} \left(G_{\text{rf}} N_{\text{th}} + N_{\text{rx, ref}} \sum_{n=1}^{N} \alpha_n^2 \right) \\ &= 1 + \frac{\sum_{n=1}^{N} \alpha_n^2}{\left(\sum_{n=1}^{N} \alpha_n \right)^2} \left[\frac{N_{\text{rx, ref}}}{G_{\text{ref}} N_{\text{th}}} \right]. \end{aligned} \tag{25}$$

Using the definition of the noise factor and receiver noise [Eqs. (10) and (12)] the bracketed term may be written in terms of the noise factor of the reference channel. The result is the noise factor of the multi-channel receiver given by

$$\text{nf}_{\text{array}} = 1 + \frac{\sum_{n=1}^{N} \alpha_n^2}{\left(\sum_{n=1}^{N} \alpha_n \right)^2} \left(\text{nf}_{\text{ref}} - 1 \right). \tag{26}$$

We see that the noise factor of the composite link is proportional to that of the reference link multiplied by the ratio of the incoherent to coherent power responses of the multiple-channel receiver. Similar to the RF gain, the improvement realized by utilizing a multiple-channel receiver will depend on the particular receiver architecture (α_n). The key point of our analysis is that the signal photocurrent combines coherently, while the noise powers are additive. In the following section we verify our analysis with two four-channel receiver architectures – one employing RF waveguide signal combination and the other employing hard-wired photodiodes.

IV EXPERIMENTAL DEMONSTRATION OF FOUR-CHANNEL ARRAYED RECEIVERS

To verify our analysis, we constructed two, 4-channel optoelectronic receivers. The general receiver architecture is shown in Figure 2 (a). The output of a single distributed feedback laser (DFB, EM4, Inc.) is modulated with a single-output low-V_π Mach-Zehnder intensity modulator (MZM, EOSpace, Inc.). The

modulator output is subsequently split evenly using a 1x4 optical coupler. Each output of the coupler is amplified using a commercial ∼30 mW EDFA (JDS Uniphase Corp.) and the input RF modulation of each channel is recovered via direct detection with a photodiode [(∼12 GHz) Discovery Semiconductor or (∼3 GHz) Applied Optoelectronics)]. The photodiode outputs are then combined either with a 1x4 RF power combiner (10 MHz - 2 GHz, M/A-COM Wilkinson power combiner), or via hard-wiring with a custom-built combining circuit. The preceding analysis compares the performance of the arrayed receiver to that of a single reference link. The reference link architecture utilized in this work is shown in Fig. 2 (b).

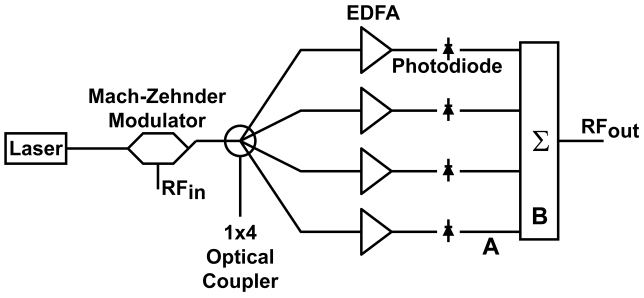

(a)

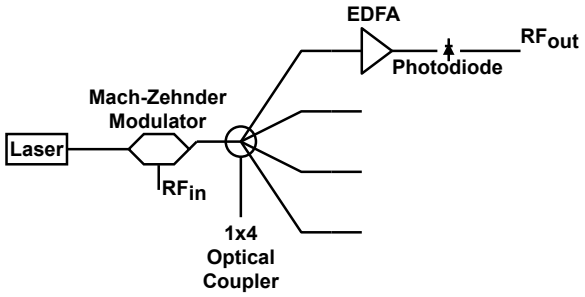

(b)

Fig. 2: (a) Intensity-modulated direct detection analog link employing a 4-channel receiver. EDFA: erbium-doped fiber amplifier. (b) Single-channel reference link architecture.

Predicted Performance

Before comparing the performance of the different receivers, it is useful to consider the theoretical improvements in RF gain and noise figure that may be achieved in these architectures and consider potential trade-offs that may affect the choice of one over the other. For the receiver employing an RF power combiner, the channel weighting (α_n) is determined by the field coupling coefficient of the combiner (assuming no excess electrical loss and that the photodiodes do not contain internal matching resistors) and is equal to [14]

$$\alpha_n = \frac{1}{\sqrt{N}}, \tag{27}$$

where N is the number of inputs to the combiner. Note, ideally one would choose the power combiner such that the number of inputs is equal to the number of available optical channels such that the coupling loss is minimized – we will return to this point later in this section. In contrast to the power combiner where coupling loss results from impedance matching of all ports, a hardwired architecture exhibits no coupling

loss. Therefore, assuming there is no per-channel excess loss, the channel weighting in the hardwired receiver is given by $\alpha_n = 1$. We may now compare the improvement in the RF gain and noise figure for each receiver architecture.

For an N-channel receiver with equally-weighted channels, we see from Eq. (8) that the gain should exceed that of a single channel [G_{ref}, see Fig. 2 (b)] by a factor of

$$\Delta\text{Gain} = \frac{G_{\text{array}}}{G_{\text{ref}}} = \left(\sum_{n=1}^{N} \alpha_n\right)^2 = N^2 \times \alpha_n^2. \tag{28}$$

In the RF power-combined architecture with $\alpha_n = 1/\sqrt{N}$ we see the gain increases linearly with the number of channels ($\Delta\text{Gain} = N$). In contrast, for the hard-wired receiver which exhibits no coupling loss ($\alpha_n = 1$) we find that the RF gain increases quadratically with the number of channels ($\Delta\text{Gain} = N^2$). The theoretical gain improvement for the RF power-combined and hardwired architectures are shown in Figure 3 (a). From Eq. (26) we see the decrease in noise figure for the N-channel receiver is given by

$$\begin{aligned} \Delta\text{Noise Figure} &= \frac{\text{nf}_{\text{array}}}{\text{nf}_{\text{ref}}} \\ &= \frac{\sum_{n=1}^{N} \alpha_n^2}{\left(\sum_{n=1}^{N} \alpha_n\right)^2} + \frac{1}{\text{nf}_{\text{ref}}} \left[1 - \frac{\sum_{n=1}^{N} \alpha_n^2}{\left(\sum_{n=1}^{N} \alpha_n\right)^2}\right]. \end{aligned} \tag{29}$$

For equally-weighted channels, the decrease in noise figure becomes

$$\Delta\text{Noise Figure} = \frac{1}{N} + \frac{1}{\text{nf}_{\text{ref}}}\left(1 - \frac{1}{N}\right). \tag{30}$$

We see that the decrease in noise figure (or, improvement in minimum detectable signal) is independent of the receiver architecture when all channels are equally-weighted. It is important to note that the realizable decrease in noise figure achieved via an arrayed receiver is a function of the per-channel noise figure (nf_{ref}). We see that for large per-channel noise figures ($\text{nf}_{\text{ref}} \gg 1$), the noise figure of the arrayed receiver improves as $\sim 1/N$ as compared to that of a single channel. However, as the noise performance of each individual channel improves the decrease in noise figure achieved via arraying deviates from the $1/N$ relation. For large channel counts the decrease in noise figure approaches $\Delta\text{Noise Figure} = 1/\text{nf}_{\text{ref}}$; this means the minimum noise figure for the arrayed receiver is $\text{nf}_{\text{array}} = 1$ (0 dB). The dependence of the noise figure improvement on channel count and per-channel noise figure is shown in Fig. 3 (b).

Our analysis shows that the increase in sensitivity (decrease in noise figure) of an N-channel receiver is independent of the particular method by which the individual channel outputs are combined. There is, however, one primary trade-off between the two architectures as implemented in the electrical domain – receiver bandwidth. For the power-combined architecture a Wilkinson power combiner (a resistively impedance-matched waveguide combiner) is utilized. These devices are inherently broadband as the device utilized in this work illustrates (the device bandwidth of 10 MHz - 2 GHz is over two decades). This is not the case for the hardwired receiver, however. Individual photodiodes effectively behave as capacitors from a circuit standpoint; a photodiode's RF bandwidth is generally $1/RC$ limited. Therefore, when multiple devices are hard-wired in parallel, the capacitance increases as N and the overall receiver bandwidth will decrease as (at least) $1/N$. Thus, the necessary bandwidth must be considered when choosing the receiver architecture. As mentioned previously, incoherent optical techniques (such as WDM) may be employed to

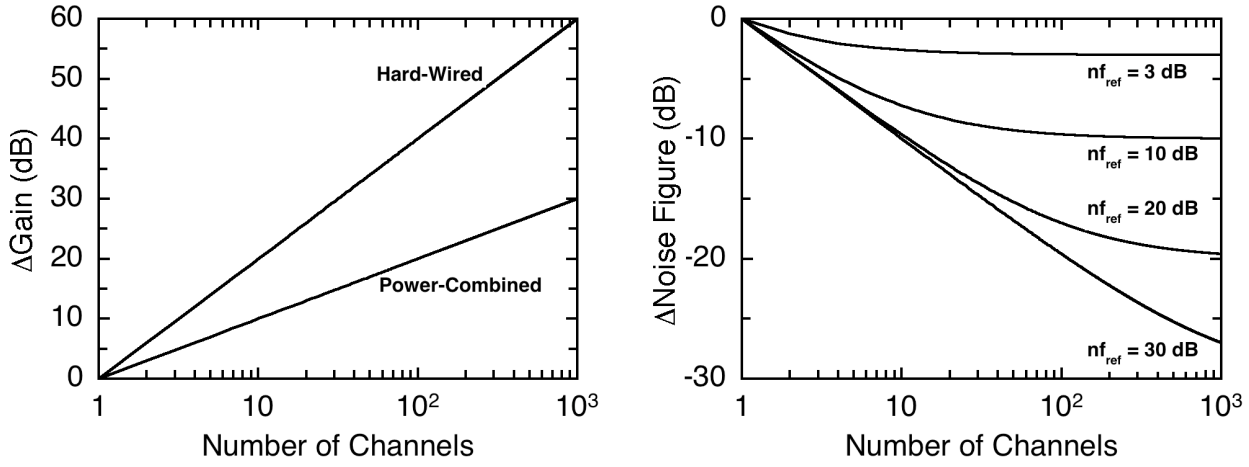

Fig. 3: Improvement in (a) RF gain and (b) RF noise figure for an N-channel receiver as a function of the number of channels. Note, the improvement in noise figure strongly depends on the noise figure of an individual channel (decreases as $1/N$ for large nf_{ref} and approaches $\Delta\text{Noise Figure} = 1/\text{nf}_{\text{ref}}$ for large N.

achieve an N-channel receiver which functions (from a mathematical perspective) identically to the hard-wired system (WDM approaches show added complexity since they requiring an N-channel transmitter). Provided a suitable photodiode is chosen (bandwidth, current handling) such architectures provide a viable alternative to the multi-diode hard-wired receiver. Though not discussed here, arrayed receivers also offer improvements in spurious-free and compression dynamic range [2, 18]; these improvements are particularly useful in cascaded systems (the analog link is one in a chain of microwave components).

Gain and Noise Penalty Characterization of Commercial EDFAs

For completeness we first characterize the performance of the EDFAs utilized in our receiver. The emphasis of our work is on the effects of EDFAs in an analog link, in particular, the noise penalty incurred by their use. Therefore, we will not spend too much time discussing measurement of the EDFA parameters. The measurement of the optical gain is a straight-forward process and the optical noise figure was measured using an established opto-electronic RIN-subtraction technique [19]. The basic idea behind this technique is to extract the additional electrical noise arising from the EDFA (N_{edfa} throughout Section III). With this quantity and the optical gain, one may calculate the EDFA noise figure and penalty from Eqs. (15) and (18), respectively.

Figure 4 shows representative values of gain, output power, and noise figure for our commercial EDFAs – as a function of input power to the amplifier – operating at a pump current of ∼300 mA (out of a maximum of 350 mA). At this pump current level, the amplifiers exhibit a maximum small-signal gain of $G_{\text{opt, max}} = 35$ dB for input powers in the range of $P_{\text{in}} <\sim -20$ dBm. The minimum noise figure is roughly $\text{NF}_{\text{opt, min}} = 3.5$ dB and is achieved for input powers in the range $-20 \lesssim P_{\text{in}} \lesssim -5$ dBm. The saturated output power of the EDFAs is $P_{\text{sat}} \approx 17$ dBm ($P_{\text{in}} \gtrsim -10$ dBm). Because we are primarily interested in the noise penalty incurred by using an EDFA, it is also useful to compare the excess electrical noise to the shot noise that would result from the use of a noiseless amplifier. Figure 5 (a) shows the total output electrical noise ($\diamond$) measured at the EDFA output as compared to the ideal shot noise level ($\circ$). For low input powers, the noise

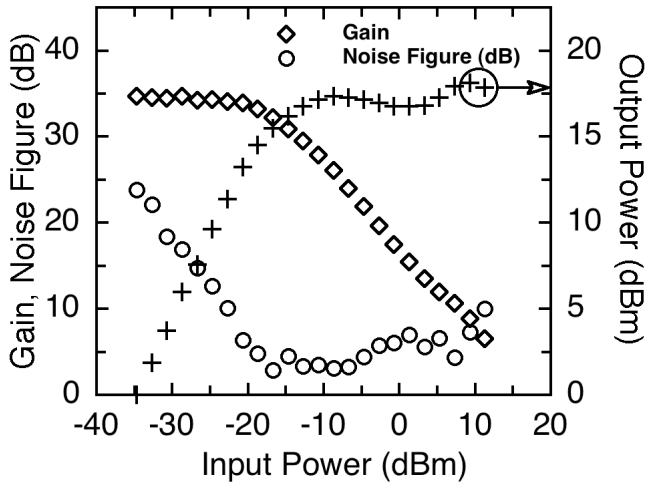

Fig. 4: Representative gain ($\diamond$), noise figure ($\circ$) and output power ($+$) curves, as a function of input power to the amplifier, for the commercial EDFAs utilized in this work.

level is dominated by the ASE from the amplifier ($P_{\text{in}} \lesssim -15$ dBm). As the input power to the amplifier is increased, beating between the amplified laser and the ASE is the limiting noise source, and when the amplifier is very heavily saturated the total noise level approaches that due to shot noise (5 dBm $\lesssim P_{\text{in}}$). Note, the laser utilized in this work is essentially shot-noise limited over the frequency range of interest [20] – this justifies setting the laser RIN in Eq. (11) to $N_{\text{laser}} = 0$. The noise penalty [Eq. (18)] calculated from the measured EDFA parameters is shown in Fig. 5 (b). The key point here is that the noise penalty arising from the EDFA may be quite large when the amplifier is operating in a linear regime and decreases toward zero as the amplifier saturates [7].

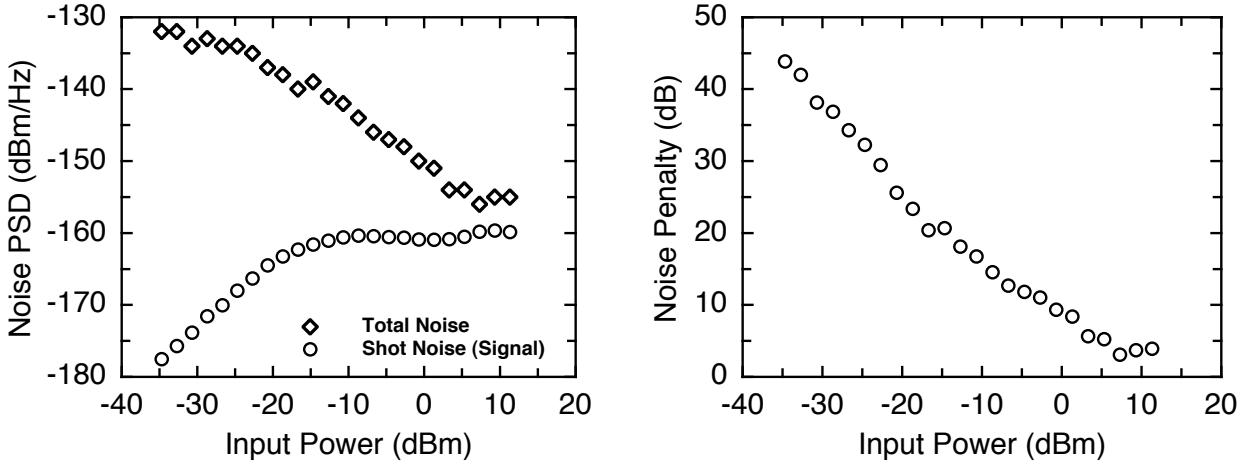

(a) (b)

Fig. 5: (a) Comparison of the total electrical output noise ($\diamond$) and the shot noise arising solely from the amplified laser (calculated, $\circ$). (b) The noise penalty of the commercial EDFA as defined by Eq. (18).

Radio-Frequency Gain and Noise Figure of Analog Optical Links Employing Multiple-Channel Receivers

We now demonstrate the performance of both the power-combined and hard-wired receiver architectures. Several parameters are common to both optical link geometries. In particular, the EDFAs are operated at 300 mA of pump current and the injected optical power per-amplifier is $P_{\text{in}} = -11$ dBm. These operating conditions yield an optical gain and noise figure of $G_{\text{opt}} = 27.3$ dB and $\text{nf}_{\text{opt}} = 3.5$ dB, respectively (see Figure 4) . Also, the same optical modulator is utilized for both links and exhibits a halfwave voltage of $V_\pi \sim 2.2$ V in the frequency range of 50 - 500 MHz. The single-channel DC photocurrent for the power-combined architecture is $I_{\text{dc, ref}} = 25$ mA and that for the hard-wired receiver is $I_{\text{dc, ref}} = 9$ mA. Note, these photocurrents are the maximum uncompressed DC photocurrents for the two types of diodes utilized in this work. These are chosen to maximize the single-channel gain for each architecture. The channel weighting of the hard-wired architecture is $\alpha_n = 1$ since there is no coupling loss in the combiner. For the RF power

Table 1: EDFA and Optical link parameters for the power-combined and hardwired receivers. The input power to each EDFA, for both link architectures is $P_{\text{in}} = -11$ dBm.

Parameter	Power-Combined	Hardwired
G_{opt} (dB)	27.3	
nf_{opt} (dB)	3.5	
V_π (V)	$\sim$2.2	
$I_{\text{dc,ref}}$ (mA)	25	9
α_n	$1/2\sqrt{2}$ $(N > 1)$	1
α_l (dB)	0	-6.8
η	0.5	0.71

combined architecture we utilize a 1x4 Wilkinson power combiner and impedance-matched photodiodes, leading to a channel weighting of $\alpha_n = 1/2\sqrt{2}$ (for two or more channels). For a single channel in the power combined architecture $\alpha_n = 1/2$ which reflects only the impedance-matched photodiode (no power combiner necessary). While there is no post-modulator optical loss in the power-combined architecture ($\alpha_l = 0$ dB) an additional $\alpha_l = -6.8$ dB loss is introduced per-channel in the hardwired architecture. This additional loss is necessary to obtain the desired DC photocurrent (which is lower than that in the power-combined architecture) while keeping the operating point of the EDFAs the same as in the power-combined architecture. Finally, the photodiode quantum efficiencies for the power-combined and hard-wired receivers approximately $\eta = 0.5$ and $\eta = 0.71$, respectively. The link and EDFA parameters are listed in Table 1.

The measured RF gain for each receiver is shown in Figure 6. For the RF power-combined architecture [Fig. 6 (a)] the single-channel gain ($\circ$) agrees very well with the predicted value of $G_{\text{ref}} = -1.0$ dB calculated from Eq. 8 using the parameters in Table 1 for a single channel. Note, the roll-off in gain at higher frequencies is due to the frequency-dependence of the modulator halfwave voltage [see Eq. (8)]. As the number of channels is increased (two channels: $\diamond$, three channels: $\square$, four channels: $\triangle$), the gain increases according to $\Delta\text{Gain} = M^2/4$, where M is the number of channels utilized and N=4 is the total number of channels [see Eq. (28)]. The power combined architecture shows a maximum improvement in gain when all four channels are utilized (this is why the combiner should be chosen to have only the number of available optical channels and no more). The improvement in gain, compared to a single channel

operating at $I_{\text{dc,ref}} = 25$ mA, for the power combined architecture is shown in Figure 7 (a). Here the measured increase in gain for two, three, and four channels ($\diamond$, $\square$, $\triangle$, respectively) agrees extremely well with the predicted values of $\Delta\text{Gain} = 0$, 3.5, and 6 dB (shown by the dashed lines). The less than 0.2 dB deviation from theory is due to slight differences in DC photocurrent and electrical frequency response between channels. In Figure 6 (b), the single channel gain ($\circ$) for the hard-wired receiver is again found to agree quite well with the theoretical value of $G_{\text{ref}} = -3.8$ dB. As the channel count (M) is increased, the gain improves as $\Delta\text{Gain} = M^2$, compared to a single channel with $I_{\text{dc,ref}} = 9$ mA. As shown in Fig. 7 (b), the improvement in gain shows excellent agreement for two, three, and four channels (two channels: $\diamond$, three channels: $\square$, four channels: $\triangle$) with the theoretical values of $\Delta\text{Gain} = 6$, 9.5, and 12 dB (shown by the dashed lines). At this point it is worth mentioning the bandwidth of the hard-wired receiver. The photodiodes utilized in this receiver have a 1/RC-limited bandwidth of 3 GHz. When four of these diodes are are combined in parallel, one should expect the receiver bandwidth to drop by at least a factor of 4. This would place the receiver bandwidth at $\sim$750 MHz. Additionally, the combination circuit itself will exhibit stray capacitance which can also be quite large – further decreasing the bandwidth. From Fig. 6 (b), we see the -3 dB bandwidth is approximately 300 MHz – an order of magnitude lower than the bandwidth of an individual diode. This fact must be addressed in the receiver design.

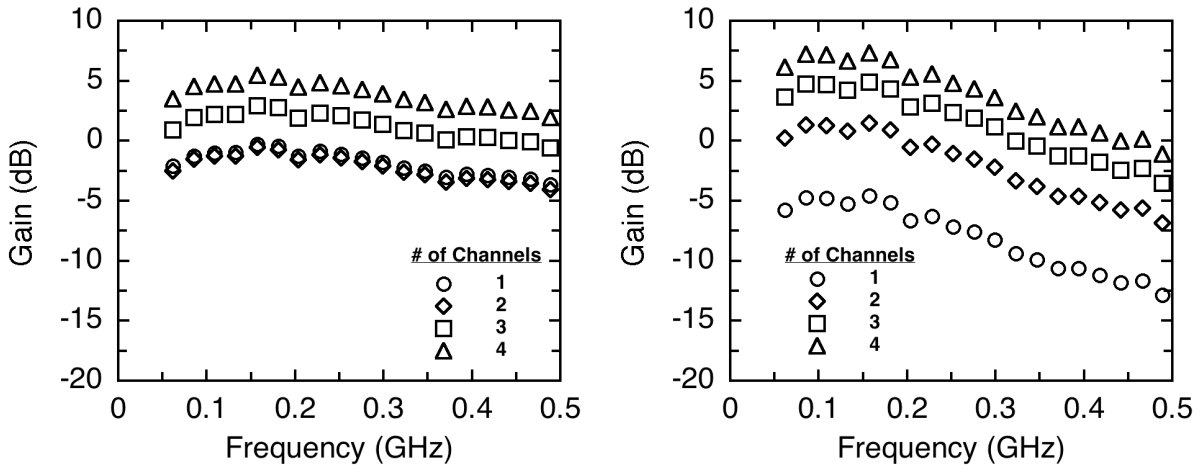

Fig. 6: RF gain as a function of frequency and number of receiver channels for (a) the power-combined architecture and (b) the 4-channel hard-wired receiver.

The measured RF noise figure for the power-combined and hard-wired receivers are shown in Figure 8 (a) and (b), respectively. For the power-combined architecture, the measured single-channel noise figure agrees exceedingly well with that calculated from Eq. (23) (shown by the solid black curve) using the EDFA parameters in Table 1 and the measured single-channel RF gain of Figure 6 (a). As expected, as the channel count is increased the noise figure decreases proportionally to $\Delta\text{nf} = 1/N$. This trend is illustrated in Figure 9 (a). Here, the measured decrease in noise figure agrees fairly well with the theoretical values of predicted by Eq. (30) of $\Delta\text{nf} =$ -3, -4.8, and -6 dB (shown by the dashed lines). The offset from the theoretical values is attributed to an $\sim$1 dB excess loss in the electrical measurement system. This conclusion is supported by the relative improvement between the two, three, and four-channel implementations – which agree extremely well with theory. The measured noise figure of the single-channel hard-wired link, shown in Fig. 8 (b) by the circles, also shows excellent agreement with the theoretical value calculated from Eq. (23) (shown by

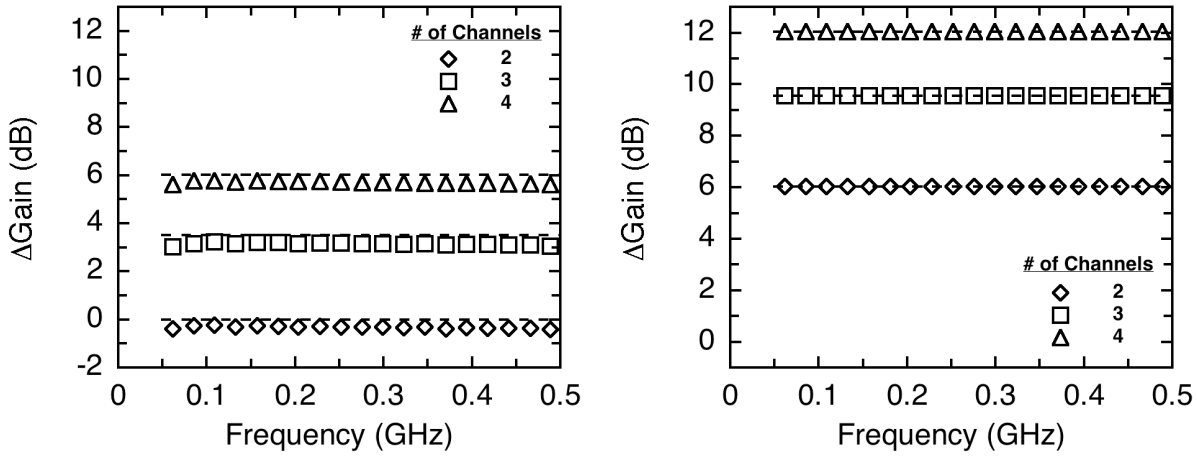

Fig. 7: Measured increase in RF gain (above that for a single receiver channel) as a function of number of receiver channels for (a) the power-combined architecture and (b) the 4-channel hard-wired receiver. In both plots, the dashed black lines show the predicted gain increase from Eq. (8) with $\alpha_n = 1/2\sqrt{2}$ for the power-combined receiver and $\alpha_n = 1$ for the hardwired receiver.

the solid black line). As shown in Figure 9 (b), as the channel count is increased to two, three, and four channels, the predicted decrease in noise figure follows the expected $\Delta\text{nf} = 1/N$ trend quite well. In all cases, the deviation from theory is less than $\sim$0.2 dB, which is within the error bounds of the measurement system.

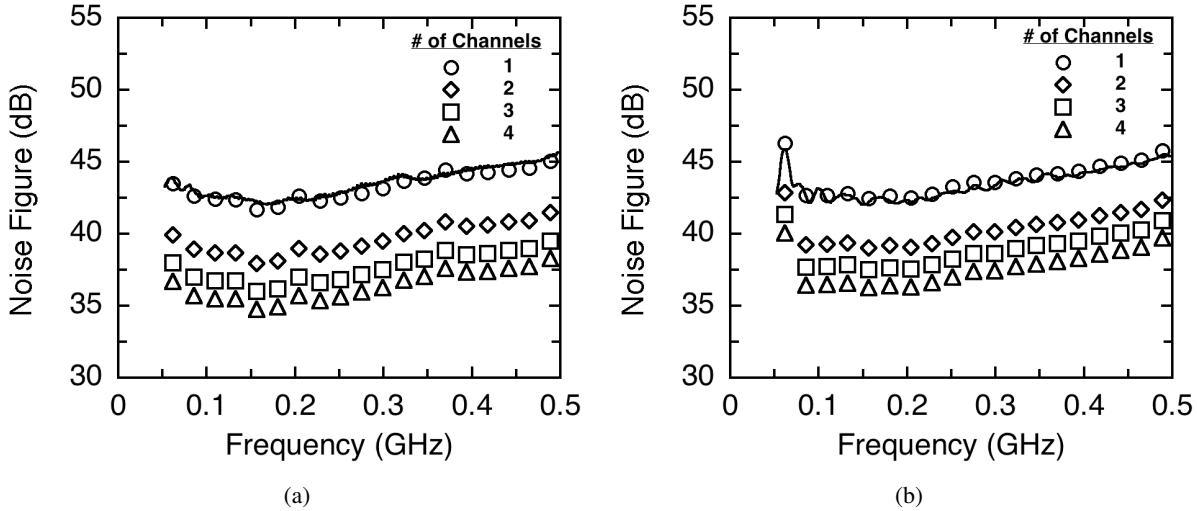

Fig. 8: Measured RF noise figure as a function of the number of receiver channels for (a) the power-combined architecture and (b) the 4-channel hard-wired receiver. For both architectures the solid black curve shows the noise figure calculated from Eq. (23) using the measured RF gain, photodiode quantum efficiency (η) and post-EDFA loss per channel (α_l).

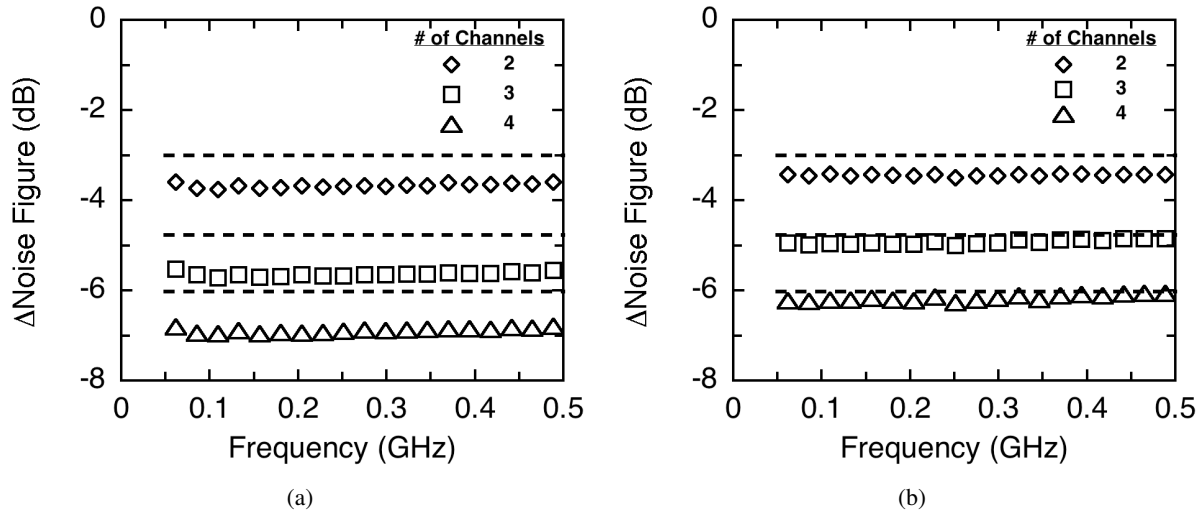

Fig. 9: Measured decrease in RF noise figure as a function of the number of receiver channels for (a) the power-combined architecture and (b) the 4-channel hard-wired receiver.

V SUMMARY

We present a detailed noise analysis of analog optical links employing multiple-channel arrayed receivers. The general receiver description developed in this work may be applied to virtually any electrically- or optically-combined receiver system - examples include RF power-combined and hard-wired receivers, as well as incoherent optically-combined architectures. In addition, we provide a general expression for the noise penalty incurred by the use of optical amplifiers in an analog link; this extends the concept of noise penalty to analog links operating at very low injected signal levels (such as free-space systems) and provides a simple method to predict the performance of an analog link based on measured parameters of an optical amplifier. Experimental results are presented for two, four-channel link architectures (power combined and hard-wired). The measured gain and noise figure are in excellent agreement with the theoretical description of the receivers. As the most complete description of arrayed receivers to date, this work provides the background necessary to construct high-fidelity arrayed receivers for fiber-based or free-space applications.

VI ACKNOWLEDGEMENT

The authors would like to thank Kristina R. Colladay and John F. Diehl for delay-matching the fiber paths in the receiver.

VII REFERENCES

[1] H. Pfrommer, M. A. Piqueras, J. Herrera, V. Polo, A. Martinez, S. Karlsson, O. Kjebon, R. Schatz, Y. Yu, T. Tsegaye, C. P. Liu, C. H. Chuang, A. Enard, F. V. Dijk, A. J. Seeds, and J. Marti, "Full-duplex docsis/wireless docsis fiber-radio network employing packaged afpm-based base-stations," *IEEE Photon. Technol. Lett.*, vol. 18, pp. 406–408, 2006.

[2] V. J. Urick, J. F. Diehl, A. S. Hastings, C. Sunderman, J. D. McKinney, P. S. Devgan, J. L. Dexter, and K. J. Williams, "Analysis of fiber-optic links for hf antenna remoting," U.S. Naval Research Laboratory, NRL Memorandum Report NRL/MR/5650-08-09101, March 2008.

[3] V. J. Urick, A. S. Hastings, J. L. Dexter, K. J. Williams, C. Sunderman, J. F. Diehl, and K. R. Colladay, "Field test on the feasibility of remoting hf antennas with fiber optics," U.S. Naval Research Laboratory, NRL Memorandum Report NRL/MR/5652–08-9137, July 2008.

[4] J. Campany, B. Ortega, D. Pastor, and S. Sales, "Discrete-time optical processing of microwave signals," *J. Lightwave Technol.*, vol. 23, no. 2, pp. 702–723, Feb. 2005.

[5] C. H. Cox III, *Analog Optical Links: Theory and Practice*. New York: Cambridge University Press, 2004.

[6] E. Desurvire, *Erbium-Doped Fiber Amplifiers: Principles and Applications*. New York: John Wiley and Sons, Inc., 1994.

[7] V. J. Urick, M. S. Rogge, F. Bucholtz, and K. J. Williams, "The performance of analog photonic links employing highly compressed erbium-doped fiber amplifiers," *IEEE Trans. Microwave Theory Tech.*, vol. 54, pp. 3141–3145, 2006.

[8] G. L. Abbas, V. W. S. Chan, and T. K. Yee, "A dual-detector optical heterodyne receiver for local oscillator noise suppression," *J. Lightwave Technol.*, vol. 3, pp. 1110–1122, 1985.

[9] K. J. Williams, L. T. Nichols, and R. D. Esman, "Externally-modulated 3 ghz fibre optic link utilising high current and balanced detection," *Electron. Lett.*, vol. 33, pp. 1327–1328, 1997.

[10] J. D. McKinney, M. Godinez, V. J. Urick, S. Thaniyavarn, W. Charczenko, and K. J. Williams, "Sub-10 db noise figure in a multiple-ghz analog optical link," *IEEE Photon. Technol. Lett.*, vol. 19, pp. 465–467, April 2007.

[11] H. V. Roussell, M. D. Regan, J. L. Prince, C. H. Cox, J. X. Chen, W. K. Burns, G. E. Betts, E. I. Ackerman, and J. C. Campbell, "Gain, noise figure and bandwidth-limited dynamic range of a low-biased external modulation link," in *2007 IEEE International Topical Meeting on Microwave Photonics*, Oct. 3–5 2007, pp. 84–87.

[12] R. J. Mailloux, *Phased Array Antenna Handbook*. Boston: Artech House, Inc., 1994.

[13] R. A. Minasian, "Photonic signal processing of microwave signals," *IEEE Trans. Microwave Theory Tech.*, vol. 54, no. 2, pp. 832–846, Feb. 2006.

[14] D. M. Pozar, *Microwave Engineering*, 3rd ed. Hoboken: John Wiley and Sons, Inc., 2005.

[15] D. M. Baney, P. Gallion, and R. S. Tucker, "Theory and measurement techniques for the noise figure of optical amplifiers," *Optical Fiber Technology*, vol. 6, no. 2, pp. 122–154, Apr. 2000.

[16] A. Yariv, *Optical Electronics*, 3rd ed. New York: Holt, Rinehart and Winston, Inc., 1985.

[17] A. Papoulis, *Probability, Random Variables, and Stochastic Processes*, 3rd ed. New York: McGraw-Hill, 1991.

[18] A. Hastings, V. J. Urick, C. Sunderman, J. Diehl, J. D. McKinney, D. Tulchinsky, P. S. Devgan, and K. J. Williams, "Suppression of even-order photodiode nonlinearities in multi-octave photonic links," *accepted for publication in the IEEE J. Lightwave Technol.*, 2008.

[19] F. W. Willems, J. C. van der Plaats, C. Hentschel, and E. Leckel, "Optical amplifier noise figure determination by signal rin subtraction," in *Symposium on Optical Fiber Measurements*, ser. NIST Technical Digest, 1994, pp. 7–9.

[20] V. J. Urick, P. S. Devgan, J. D. McKinney, and J. L. Dexter, "Laser noise and its impact on the performance of intensity-modulation direct-detection analog photonic links," U.S. Naval Research Laboratory, NRL Memorandum Report NRL/MR/5652-07-9061, 2007.

APPENDIX A

VIII APPENDIX-A: SIMULATION CODE FOR CALCULATION OF THE GAIN AND NOISE FIGURE OF AN N-CHANNEL ARRAYED RECEIVER

This code takes a user-defined 2-dimensional spatial power profile (beam shape) and assumes it is incident on an NxN array of optical receivers, each containing an EDFA. Note, the spatial coordinates (X,Y) refer to array position in an NxN array [(0,0) taken at center]. Given the peak incident power, the output optical power and noise penalty is calculated for each receiver, and the overall array gain and noise figure are calculated by appropriately summing the signal and noise components across the array. Calculations / variables are referenced back to the relevant equations in the text.

There are several assumptions in this code:

1. The optical gain and noise penalty are specific to the JDS OA400 operating at a pump current of 300 mA and a signal wavelength of 1555 nm. As there are significant variations (particularly in the optical noise figure) with wavelength and pump current, different operating conditions or different amplifiers may give significantly different results. The parameters for other EDFAs, however, may be easily inserted.

2. The optical amplifier is assumed to be operating in the linear (unsaturated) regime. The optical gain is taken to be a constant, and the optical noise figure is a numerical fit based on measured data for the OA400. This assumption will be valid for typical free-space applications employing the OA400.

3. A hard-wired receiver is assumed (there is no coupling loss included) since the particular electrical combination technique does not affect the decrease in receiver noise figure. To model a power-combined architecture, the receiver gain (in dB) should be reduced by a factor of $10 \log\left(1/N^2\right)$.

4. The photodiodes are assumed to have no internal impedance matching resistor. Again, this does not affect the noise figure. To adjust the gain (in dB), reduce by 6 dB (maximum power transfer).

Link Parameters

Variable	Definition	Value
nu	Optical Frequency	192.9e12 (Hz)
Ri	Modulator resistance	50 (Ω)
Ro	Load resistance	50 (Ω)
kT	Thermal noise PSD	$10^{(-174/10)}$ (mW/Hz)
Vp	Modulator halfwave voltage	2 (V)
eta	Photodiode quantum efficiency	.7 (unitless)

Input Variables

The user is prompted for these.

Variable	Definition
Po	Maximum received optical power (in mW).
N	number of receiver elements in one dimension.
F	spatial power distribution. Function of variables X & Y.

Output Variables

Variable	Definition
Gain_Array	Receiver gain
NF_Array	Receiver noise figure

Intermediate Variables

The following are (mostly) element-by-element values utilized in the code. These are useful if you want to look at various parameters of individual elements in the receiver array.

Variable	Definition
Pin	Spatial power profile (in mW)
nfo	Optical noise figure of each EDFA
Go	EDFA gain (34 dB)
npo	Optical noise penalty of each EDFA
Idc	Maximum DC photocurrent
Idc_Element	Per-element DC photocurrent
Gref	Gain of the reference link (using max. Idc)
Gain_Element	Per-element RF gain
Noise_Element	Per-element noise PSD (mW/Hz)
Nrx_Element	Per-element receiver noise PSD (mW/Hz)
NF_Element	Per-element noise figure (dB)
Noise_Array	Total receiver noise PSD (mW/Hz)

```
%NArray.m
%
% This program calculates the Gain and Noise Figure for an analog optical
%link employing an NxN arrayed receiver.
% Jason D. McKinney 11-September, 2008
%
%
%
clear
clc
close all;
%
% Variable Definitions
q = 1.619e-19;      % Electronic charge (C)
h = 6.626e-34;      % Planck's Const. (J-sec)
nu = 3e8 / 1555.2e-9; % Optical Freq. (Hz) - Assumes 1555.2 nm wavelength
Ri = 50;            % Modulator input resistance (Ohms)
Ro = 50;            % Load resistance (Ohms)
kT = 10^(-174/10);  % Thermal noise (mW/Hz) - assumes 290 K
Vp = 2;             % Modulator halfwave voltage (V)
eta = .7            % Photodiode quantum efficiency (unitless)
R = eta*q/h/nu;     % Photodiode responsivity (A/W)
%
%
Po = input('Enter maximum optical power (in mW): ');    % Define peak input
                                                        % power
% Define array size and position coordinates
N = input('Enter array linear dimension: '); % Assumes a square array
x = -N/2:1:N/2 - 1;
y = x;
[X,Y] = meshgrid(x,y);
%
% Enter spatial power distribution (normalized to 1)
F = ...
input('Enter spatial power distribution [e.g., exp(-((X).^2 +(Y).^2))]: ');
% Define actual power distribution
Pin = Po*F;
%
%EDFA Parameters
% - These are functional fits the measured gain / noise figure of a
% JDS Uniphase OA400, pumped at 300 mA, for a center wavelength of
% 1555.2 nm. Note, these assume the amplifier is operating in the linear
% gain regime (input powers below -20 dBm in Fig. 4 of the report). For a
% different amplifier, these will change!
%
nfo = 2.71e-2 * 1./(Pin.^1.138);    % Optical Noise Factor (unitless)
Go = 10^(34/10);                    % Optical Gain (unitless)
```

```
npo = Go.*nfo;  % Noise penalty [Eq. (20)] defined
                                    % across the receiver array (unitless).

% Analog Link Calculations
%
 Idc = R*Po.*Go.*max(max(F));    % Maximum DC photocurrent of the receiver
                                 % array (mA). This will be the reference
                                 % photocurrent, used to calculate the
                                 % reference gain [see Eq. (8)].
%
Idc_Element = R*Po.*Go.*F;       % DC current distribution for each link of
                                 % the array (mA).
%
Gref = (pi*Idc*1e-3 / Vp)^2 * Ri * Ro;  % Gain of the reference link
                                        %(unitless)
%
Gain_Element = Gref.*F.^2;     % Gain of each link in the array (unitless).
%
%
% Total RF Gain (dB) [Eq. (8)]. Note, if you want the gain for a
%power-combined architecture, reduce this value by 10*log10(1/N).
%If you want to predict the gain for a link using impedance-matched
%photodiodes, reduce this value by 6 dB.
Gain_Array = 10*log10(sum(sum(F))^2 * Gref)

%Noise_Element = Output thermal + amplified input thermal
%                + shot noise + EDFA noise.
Noise_Element = ((kT*(1+Gain_Element) ...
    + 2*q*50*Idc_Element.*((1-eta) + eta*Go*nfo))) ;     % Noise PSD for
                                                         % each receiver
                                                         % independently
                                                         % (mW/Hz)
                                                         % [Eq. (11)]
%
Nrx_Element = Noise_Element - kT;   % RX noise PSD per element (mW/Hz).
%
% RF Noise Figure for each link in the array, independently (dB)
% [general noise figure definition of Eq. (10) including input / output
% thermal noise, shot noise, and EDFA noise.
NF_Element = 10*log10(1+1./Gain_Element+Noise_Element./Gain_Element/kT);
%
%Total Noise PSD (mw/Hz) of the arrayed receiver. The first term is
%amplified input thermal noise for each link in the array. The second term
%is the total receiver noise of the array.
Noise_Array = sum(sum(kT*Gain_Element)) + sum(sum(Nrx_Element));
```

```
%Noise Figure of the arrayed receiver (dB). [general noise figure
%definition of Eq. (10) including input / output thermal noise,
%shot noise, and EDFA noise.
NF_Array = 10*log10(1+ 1/10^(Gain_Array/10) ...
    + Noise_Array/10^(Gain_Array/10)/kT)
```

APPENDIX B

IX APPENDIX-B: ORDER-OF-MAGNITUDE ANALYSIS OF THE EXCESS NOISE ARISING FROM INCORPORATION OF AN EDFA

In Section III we make the assumption that the excess noise added by the EDFA may be approximated by the sum of signal-ASE and ASE-ASE beat noise and that the additional shot noise arising from the total ASE power may be safely ignored. To justify this assumption, we must compare the relative magnitudes of these three noise components. From [15], the intensity noise spectral densities (W^2/Hz, PSD normalized to $\alpha^2 R_o$) of the signal-ASE ($S_{\text{s-ase}}$) and ASE-ASE ($S_{\text{ase-ase}}$) beat noise terms are given by

$$S_{\text{s-ase}} = 4P_s\rho_{\text{ase}} \tag{31}$$

and

$$S_{\text{ase-ase}} = 4P_{\text{ase}}\rho_{\text{ase}}. \tag{32}$$

Here, P_s is the amplified laser power (W), P_{ase} is the total ASE power (W, integrated across the optical bandwidth B_o), and $\rho_{\text{ase}} = P_{\text{ase}}/B_o$ is the ASE PSD (W/Hz). The shot noise intensity spectral density (due to the total ASE power P_{ase}) is given by

$$S_{\text{shot}} = \frac{2q\alpha P_{\text{ase}} R_o}{\alpha^2 R_o} = \frac{2h\nu}{\eta} P_{\text{ase}}. \tag{33}$$

The total excess intensity noise spectral density may then be written as

$$\begin{aligned} S_{\text{excess}} = S_{\text{s-ase}} + S_{\text{ase-ase}} + S_{\text{shot}} &= \rho_{\text{ase}} \left(4P_s + 4P_{\text{ase}} + \frac{2h\nu}{\eta} \frac{P_{\text{ase}}}{\rho_{\text{ase}}} \right) \\ &= \rho_{\text{ase}} \left(4P_s + 4P_{\text{ase}} + \frac{2h\nu}{\eta} B_o \right) \end{aligned} \tag{34}$$

For a C-band EDFA (1530-1565 nm) without an optical filter, the ASE bandwidth is approximately $B_o = 4$ THz. The quantity $2h\nu/(\eta B_o)$ at a center wavelength of 1550 nm is then approximately 1 μW. For comparison, the maximum total ASE power for the OA400 is $P_{\text{ase}} \approx 20$ mW. The output signal power can obviously vary from zero to the saturated output of the EDFA. So, for a fixed ASE power (equivalently, fixed power spectral density) the shot noise contribution to the excess noise is roughly *four orders-of-magnitude* smaller than the sum of the beat noise components. Therefore, this shot noise term may be safely ignored in optical or electrical noise factor calculations.